EXPERIMENTAL OBSERVATIONS AND NUMERICAL SIMULATIONS OF A FREE-SURFACE VORTEX IN A TEST VESSEL

Aljaž ŠKERLAVAJ*

University of Trieste, Department of Engineering and Architecture, Italy; currently on leave from Kolektor Turboinštitut d.o.o., Slovenia

Darko ERMENC

Pumps Department, Kolektor Turboinštitut d.o.o., Slovenia

ABSTRACT

The paper presents a comparison between experimental observation and numerical prediction of a free surface vortex in a cylindrical test vessel. The Reynolds number for the outlet pipe was above 60,000, according to the recommendations of the standard for pump sump testing. In particular, the length of the free-surface gas core and the downward velocity inside the vortex were compared. The simulation was performed as a single-phase simulation. The length of the gas core was estimated in the post-processing phase, based on the local field variables at the vortex core near the water surface and on the assumption of the Burgers vortex type. The numerically predicted velocity inside the vortex core was compared to the travelling velocity of injected dye. Based on the obtained CFD results it is possible to conclude that the presented technique is a promising one for estimation of gas core length of free-surface vortices, even at Reynolds number 60,000.

KEYWORDS

free-surface vortex, CFD, pump intake, experimental vessel

1. INTRODUCTION

Free-surface vortices appear in various engineering systems, where they can have detrimental effects. In case of nuclear reactor vessels with liquid surface (e.g. sodium-cooled fast-breeder reactors (SFBR)) they cause fluctuations in reactivity due to the void effect. In case of pump intakes, free-surface vortices cause increased noise, vibrations, and possibly even failure of the pump. The general tendency of design, including design of reactor vessels and pump intakes, is to reduce size of the systems, which leads lo larger velocities and consecutively to stronger vortices.

During research related to Japanese SFBR feasibility studies, several vortex test vessels were created in order to develop design criteria for the prediction of gas entrainment from vortex dimples. For a vortex test vessel, designed by Monji et al. [1], Reynolds number (based on the outlet pipe diameter and corresponding average velocity) reached 13,000. In case of Moriya's

* *Corresponding author:* Turbines Department, Kolektor Turboinštitut d.d., Rovšnikova 7, Ljubljana, Slovenia, phone: +386 1 5820152, email: aljaz.skerlavaj@turboinstitut.si

test vessel [2], Reynolds number reached approximately 42,000. The standard for pump intake experimental testing [3] prescribes that tests should be performed at Reynolds number higher or equal to 60,000 in order to reduce uncertainties due to the scale up to the prototype size.

Numerical simulations can be performed with various levels of accuracy. Although numerical simulations can be performed by using two-phase modelling and large-eddy-simulation (LES) (as a turbulence model), such simulations are not suitable for engineering purposes. It is more convenient to use single-phase simulations with two-equation Reynolds-averaged Navier-Stokes (RANS) turbulence models. The gas-core length of the free-surface vortex is then obtained in a post-processing phase by assumption of the vortex-type model (e.g., Burgers vortex).

In the paper an experimental vessel of free-surface vortex is presented. The Reynolds number of the vessel (based on the outlet pipe diameter and corresponding average velocity) is approximately 60,000, which is in accordance with the recommendations in [3]. The gas-core length of free surface vortex shows stable behaviour even for long gas cores. Single-phase numerical simulations were performed. Numerically predicted gas-core length and downward velocity of a vortex are compared to experimental results.

2. EXPERIMENTAL AND NUMERICAL MODEL

The vortex test vessel geometry (Fig.1) was designed to achieve the value 60,000 for the Reynolds number $\mathrm{Re}_d = (Qd)/(\nu A_d)$, where Q is the volumetric flow rate, d the diameter of the outlet pipe, A_d the cross-section surface of the outlet pipe and ν the kinematic viscosity of water. Diameter of the vessel D is equal to 150 mm, the width of the inlet channel W is 40 mm, distances x and y are equal to 10 mm, and the diameter d of the outlet pipe is equal to 10 mm. In case of experimental model, the length l was equal to 1.5 m (until the nearest of the three flow straighteners). In case of numerical model, the channel was simulated separately (to obtain the inlet velocity profile), so the length l was equal to 150 mm and the length of the channel was 3 m. The length of the outlet pipe in case of numerical model was equal to 200 mm. The height H of the numerical model corresponds to the level of water surface for a corresponding experimental observation.

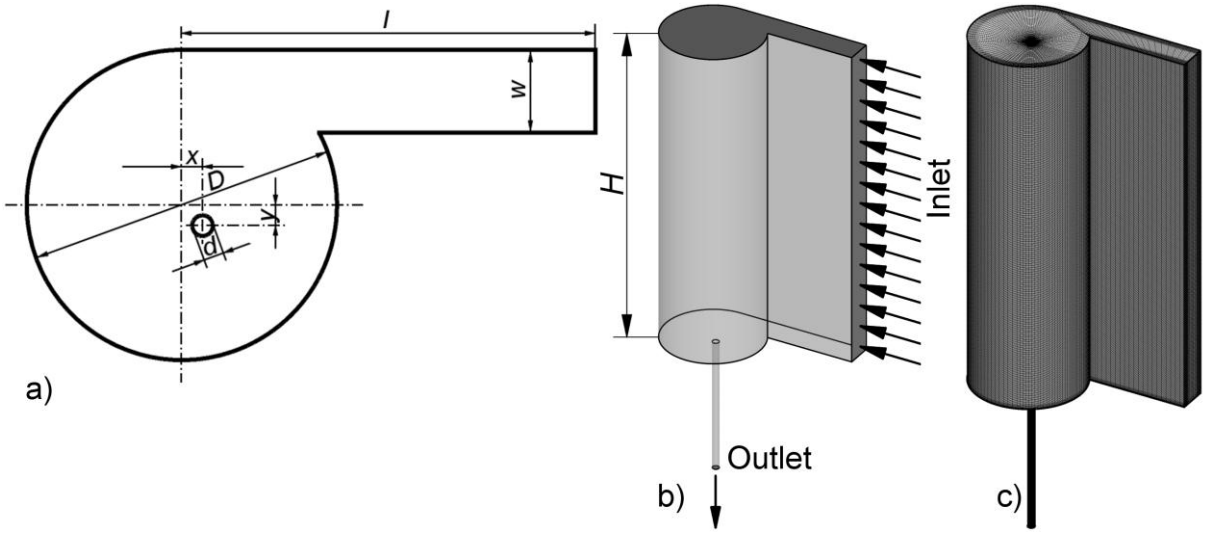

Fig.1 Test case geometry: (a) top view; (b) iso-view; (c) numerical mesh.

Water enters into the vessel through the channel, rotates in the cylindrical section and exits the vessel through a narrow pipe. A combined effect of rotation in the vessel and high

velocity through the outlet pipe creates a free-surface vortex (Fig.2a) with the gas core length L_{gc}.
The experimental vessel was designed in transparent plexiglass to enable the observations (of L_{gc} and downward velocity in the vortex). The downward velocity was observed by using injected dye (Fig. 2b) and a camera CANON EOS D60 with 50fps video mounted on a tripod. The error of light refraction was minimised by using an immersed measuring tool at the place of the vortex prior to conducting the observations. The relationship between L_{gc}, H and Q is presented in Fig.2b.

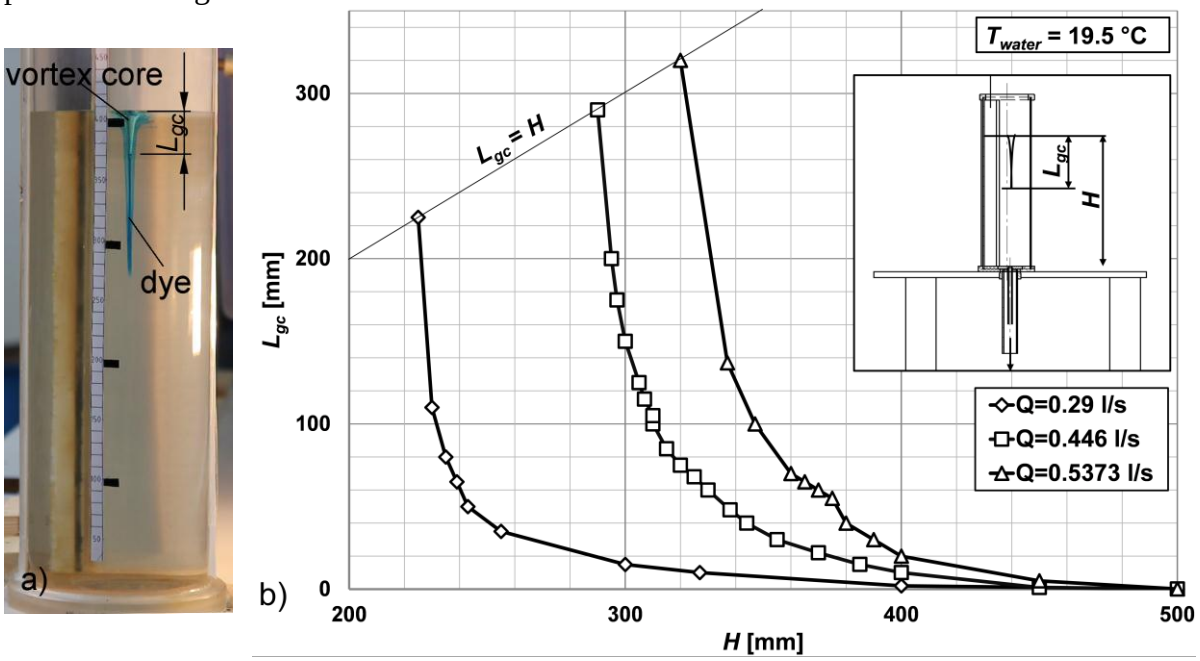

Fig.2 Experimental observations: (a) free-surface vortex and injected dye; (b) Observed relationship between gas core length of free-surface vortex(L_{gc}), flow rate Q and vessel height H.

Two operational points with Q=0.5373 l/s (Re_d=67,350) were simulated. The Case 1 was determined by H=0.483 m and L_{gc}=7.2 mm. The Case 2 was determined by H=0.4066 m and L_{gc}=40.9 mm. It should be mentioned that the L_{gc} of Case 2 is higher than presented in Fig.2b because length of the gas core was slightly varying with time. The L_{gc} of Case 2 is based on the moment the dye was injected into water to measure the downward velocity.
A block-structured mesh was used for numerical model. It consisted of 5 and 4.4 million nodes for Case 1 and Case 2, respectively. The average $y+$ on the cylindrical walls was approximately 2.5, whereas on other walls it was smaller (for Case 2). At surface, the height of the first row of elements was 0.3 mm (with geometric increase ratio 1.3). At the vessel bottom, the height of the first row of elements was 0.002 mm (with geometric increase ratio 1.3). In the vertical direction, 404 nodes were used (the largest element was 1 mm high). In the radial direction on the vessel floor, 66 nodes were used (the largest element size was 3.9 mm). In circumferential direction, the size of the elements at the cylindrical wall was 5 mm. Inside the outlet pipe, the largest side of a 2D element in a horizontal plane was 0.2 mm, whereas the element height was the largest at the outlet surface, 2mm. For Case 1, the numerically predicted vortex position at vessel surface matched the region of the highest mesh density (as visible in Fig.1c on the vessel surface) well, which means that the vortex core was represented with many (above 30) cells in each direction. For case 2, the numerically predicted vortex position at vessel surface did not match the position of the highest mesh density. In Case 2, the vortex core was represented by 11 to 12 elements in each direction, whereas the diameter of the vortex core was approximately 9.5 mm.

Single-phase transient simulations were performed. As shown in [4], it is crucial to use the curvature correction (CC) option [5] inside the RANS-based model. Therefore, the scale-adaptive-simulation shear-stress-transport turbulence model [6] with curvature correction (SAS-SST-CC) was used as a turbulence model. At the outlet, average pressure field was prescribed. Symmetry boundary condition was used at the water surface. At the inlet, a velocity profile was prescribed from the previously calculated channel-flow simulation. For Case 2, three channel simulations were performed on a 22-million mesh channel to determine the correct velocity profile: a laminar simulation, a gamma-theta transition model simulation [7] and a simulation with the SST model [8]. As it was expected from the design phase, the flow in the channel is laminar. In the simulations of the vessel, a bounded central-difference scheme was used as an advection scheme, whereas the second-order backward Euler transient scheme was used as a time-stepping scheme. In both cases, the residuals were of identical magnitude: the RMS residuals were below $2.5 \cdot 10^{-4}$, whereas the maximal residuals were below $4.5 \cdot 10^{-2}$. Statistical averaging for Case 1 was performed from 70 s until 127.5 s in 0.5 s time-steps. Time averaging for Case 2 was performed from 100 s until 127.5 s in 0.5 s time-steps. In both cases, the time-averaging started when downward velocity and length of the free-surface gas core reached converged values.

3. EXPERIMENTAL AND NUMERICAL RESULTS

In case of the single-phase numerical simulation, the length of the free-surface gas core (L_{gc}) is determined in the post-processing phase, based on the field variables at the water surface. Prediction of L_{gc} is based on a Burgers vortex model. The basic equation does not include the surface tension and is determined by the method first described in [9]

$$L_{gc} = \frac{\ln 2 \cdot \alpha \Gamma_{\infty}^{2}}{4 g \nu \left(2\pi\right)^{2}}, \tag{1}$$

where α is the downward-velocity gradient, Γ_{∞} the circulation of the vortex, ν kinematic viscosity and g acceleration due to gravity. The circulation of a given curve c (e.g. with a constant radius) around a pivot point can be assessed easily by using

$$\Gamma = \omega_z A_{z,c}, \tag{2}$$

where ω_z is component of vorticity in vertical (z axis) direction and $A_{z,c}$ is the area of water surface, bounded by the given curve. In our case, the Γ_{∞} was determined as the maximal value of the circulation in the range between the vortex radius r_0 and twice the radius [4]. In order to compute the downward velocity gradient inside the vortex core, it is necessary to define the vortex core. The most convenient method is to represent the vortex cores by iso-surface of Q invariant ($Q=0\ s^{-2}$). Then, the α inside the vortex core can be determined from radial velocity (as described in [4]), but it is even easier obtained from the relation

$$\alpha = \frac{\Delta \overline{v_z}}{\Delta z} = \frac{Q_{side}}{\Delta z \cdot A_{bottom,Q0}}, \tag{3}$$

where $\Delta \overline{v_z}$ is the difference in the average downward velocity inside the vortex core at two levels (e.g. at water surface and at distance Δz below the surface), $A_{bottom,Q0}$ is the bottom of the two surfaces, and Q_{side} is the flow rate through the side surface of invariant Q=0 (with height Δz). Since the flow is incompressible, the flow rate Q_{side} could be replaced by flow rate Q_{bottom} through surface $A_{bottom,Q0}$.

The experimental and numerical (CFD) results for downward velocity and for the length of the free-surface gas core are presented in Fig.3 and Fig.4, respectively. In case of downward velocity, CFD results are represented with time-averaged, minimal and maximal values. Similarly, the error bars in Fig.4 represent minimal and maximal values of time averaging.

For Case 1 ($L_{gc,exp}$=7.2 mm), the agreement between numerical end experimental results in Fig.3 and Fig.4 is very good. The Q_{side} and Q_{bottom} are almost equal, which means that numerically predicted L_{gc} using both values are almost identical. For Case 2 ($L_{gc,exp}$=40.9 mm), the agreement between numerical end experimental results in Fig.3 and Fig.4 are decent. It should be mentioned that for some reason the Q_{side} and Q_{bottom} were not equal, which means that numerically predicted L_{gc} was considerably different for the two values. Although it seems that Q_{bottom} was a better choice, a further investigation is needed about the reason for the difference between the Q_{side} and Q_{bottom}.

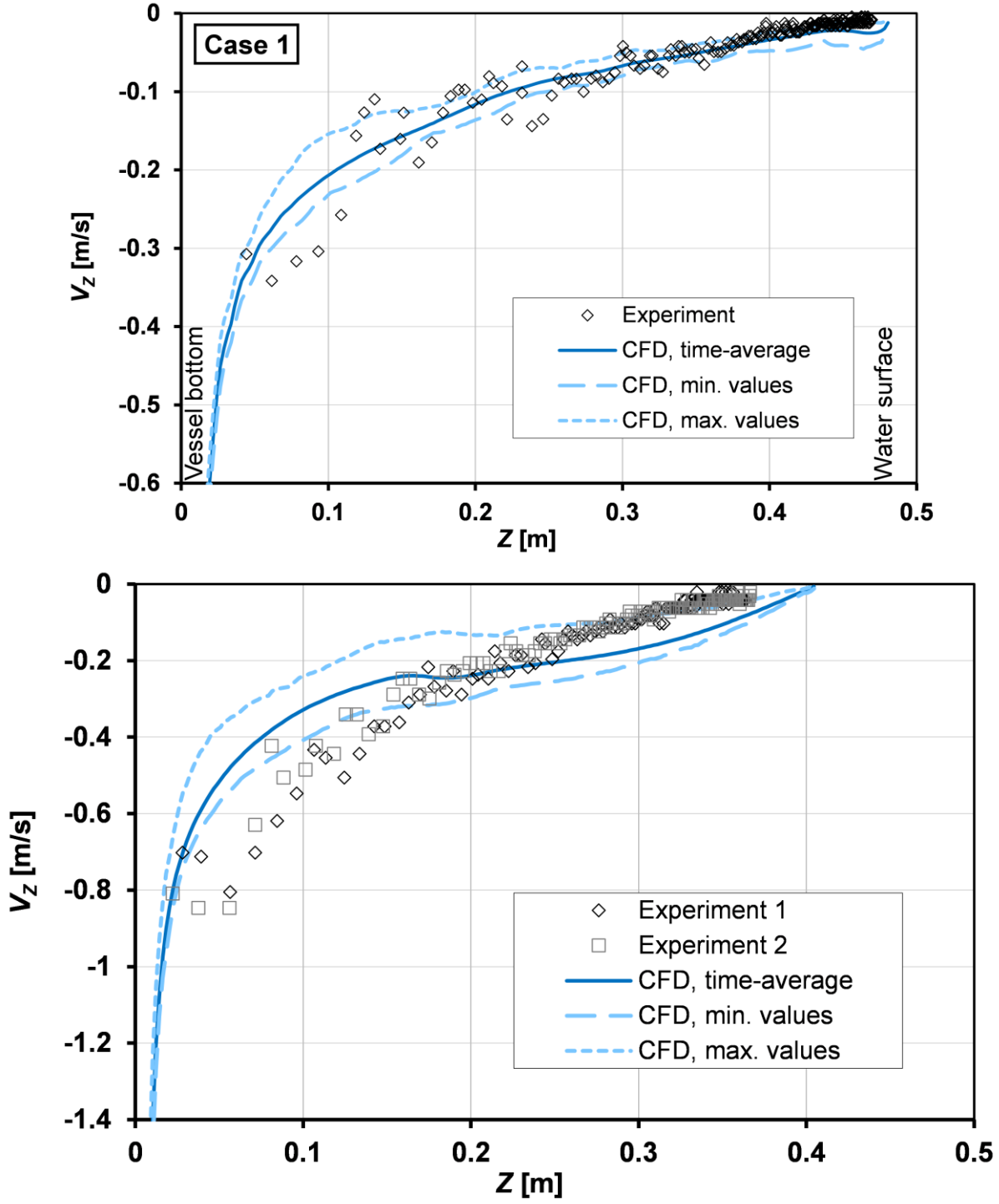

Fig.3 Experimental and numerical comparison of downward velocity; (top) Case 1; (bottom) Case 2.

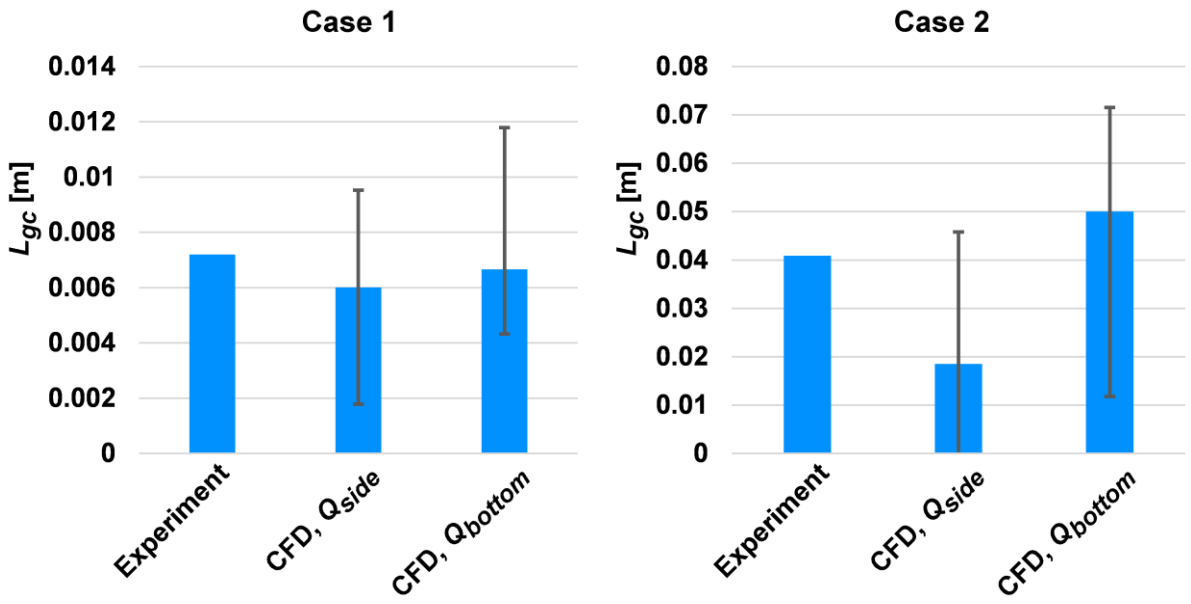

Fig.4 Experimental and numerical comparison of length of free-surface vortex gas core. (left) Case 1; (right) Case 2.

4. CONCLUSIONS

The study presents experimental results for free-surface vortex in a test vessel at Reynolds number above 60,000, which is a demand of the standard for pump intake design [1]. A CFD method for prediction of length of the free-surface gas core (L_{gc}) from a single-phase simulation was presented. The following conclusions can be made:

- for small L_{gc}, the agreement between experiment and CFD is very good;
- for larger L_{gc}, the agreement between experiment and CFD is still good, but some inconsistencies between flow rates Q_{side} and Q_{bottom} appeared, which will need further investigation.

In general, it can be concluded that the presented method is applicable at Reynolds number larger than 60,000.

5. ACKNOWLEDGEMENTS

The research leading to these results has received funding from the People Programme (Marie Curie Actions) of the European Union's Seventh Framework Programme FP7/2007-2013/ under REA grant agreement n°612279 and from the Slovenian Research Agency ARRS - Contract No. 1000-15-0263.

6. REFERENCES

[1] Monji, H., Shinozaki, T., Kamide, H. and Sakai T.: Effect of experimental conditions on gas core length and downward velocity or free surface vortex in cylindrical vessel. *Journal of Engineering for Gas Turbine and Power*. Vol. 132. 2010. pp. 012901: 1-8.

[2] Moriya, S.: *Estimation of hydraulic characteristics of free surface vortices on the basis of extension vortex theory and fine model test measurements*. CRIEPI Abiko Research Laboratory Report, No. U97072. 1998. (in Japanese).

[3] ANSI/HI. *American National Standard for Rotodynamic Pumps*. Parsippany: Hydraulic Institute. 2012.

[4] Škerlavaj, A., Škerget, L., Ravnik, J. and Lipej, A.: Predicting free-surface vortices with single-phase simulations. *Engineering Applications of Computational Fluid Mechanics*. Vol. 8(2). 2014. pp. 193–210.

[5] Smirnov, P. E. and Menter, F.: Sensitization of the SST turbulence model to rotation and curvature by applying the Spalart-Shur correction term. *Journal of Turbomachinery*. Vol. 131(4). 2009. pp. 041010-8.

[6] Egorov, Y. and Menter, F.: Development and application of SST-SAS turbulence model in the DESIDER project. *Advances in Hybrid RANS-LES Modelling* (eds. S-H Peng and W Haase). Heidelberg: Springer. 2008. pp 261-270.

[7] Langtry, R. B. and Menter, F.R.: Transition Modeling for General CFD Applications in Aeronautics. *43rd AIAA Aerospace Sciences Meeting and Exhibit*. 2005. AIAA paper 2005-522.

[8] Menter, F. R., Kuntz, M. and Langtry, R: Ten years of industrial experience with the SST turbulence model. Turbulence. *Heat and Mass Transfer 4* (eds. K Hanjalić, Y Nagano and M Tummers). New York: Begell House. 2003. pp. 625-632.

[9] Sakai, T., Eguchi, Y., Monji, H., Ito, K. and Ohshima, H.: Proposal of design criteria for gas entrainment from vortex dimples based on a computational fluid dynamics method. *Heat Transfer Engineering*. Vol. 29(8). 2008. pp. 731-739.